

Received December 21, 2018; reviewed; accepted March 12, 2019

## Atomic scale study of silver sulfide leaching with cyanide and thiourea

Roxana Bernaola-Flores <sup>1</sup>, Dhamelyz Silva-Quiñones <sup>1</sup>, Perla B. Balbuena <sup>2</sup>, Juan Carlos F. Rodríguez-Reyes <sup>1</sup>, Francisco Tarazona-Vasquez <sup>1</sup>

<sup>1</sup> Department of Bioengineering and Chemical Engineering, Universidad de Ingeniería y Tecnología - UTEC, Barranco, Peru

<sup>2</sup> Artie McFerrin Department of Chemical Engineering, Texas A&M University, College Station, Texas, USA

Corresponding author: [ftarazona@utec.edu.pe](mailto:ftarazona@utec.edu.pe) (Francisco Tarazona-Vasquez)

**Abstract:** Understanding of atomic scale interactions of molecular species with mineral surfaces is needed to bring about mineral processing innovation. In this regard, Density Functional Theory (DFT) methods are well suited. In this work, the outcome of leaching synthetic acanthite - a surrogate for a silver-containing sulfide ore- with both cyanide ion and thiourea are studied with DFT considering solvent effects. The results are correlated to the experimental percentage of silver extracted with each of the leaching agents under similar conditions of molar concentration, temperature and percentage of solids. Our calculations show both leaching reactions to be exergonic and of the same order of magnitude in Gibbs energy of reaction than values determined from thermodynamic tables. Also, less favorable Gibbs reaction energies are obtained for cyanidation in absence of oxygen and thiourea in absence of Fe(III) highlighting the impact of oxidants on the exergonicity of the respective global leaching reactions. Finally, analyzing the percentage of silver extracted from acanthite and the absolute value of Gibbs energies of the respective reaction, we conclude that the more exergonic a leaching reaction, the higher percentage of silver is extracted from acanthite, provided that there is no kinetic control of each of the leaching reactions.

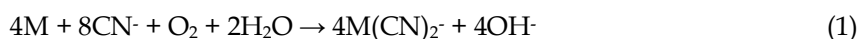
**Keywords:** leaching, cyanidation, thiourea, DFT, cluster models, Ag<sub>2</sub>S

### 1. Introduction

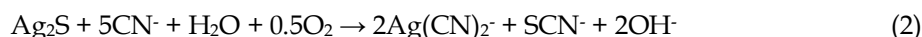
Silver is an essential precious metal in modern society for uses in jewelry, coinage, microelectronics and catalysis. Recent burn-off estimates show a worldwide shortage of silver around 2075 (Sverdrup et al., 2014). However, years before such shortage hits the market, it is likely that the easily recoverable ores are already extracted leaving behind ores refractory to conventional hydrometallurgical methods (La Brooy et al., 1994; Aylmore et al., 2001). This fact has already been observed for noble metals (Lindstrom et al., 1973; Açma et al., 1993; Celep et al., 2011; Saba et al., 2011; Alp et al., 2014; Qiu et al., 2014).

Leaching is a complex hydrometallurgical unit operation whose basic principle consists in dissolving a chemical substance –the leaching agent- in water, so such solution is able to remove a valuable metal –e.g. silver- from the mineral matrix. This is commonly done with the help of an oxidant driving the reaction through a redox reaction mechanism. Silver is found in over 200 mineral phases (Gasparrini, 1983) whether as isolated metal (native silver), alloy (i.e. electrum), sulfide (i.e. acanthite, Ag<sub>2</sub>S) or sulfosalt (i.e. freibergite, Ag<sub>6</sub>Cu<sub>4</sub>Fe<sub>2</sub>Sb<sub>4</sub>S<sub>13</sub>). It can also be accompanied by other minerals such as galena, pyrite and pyrrhotite, among others.

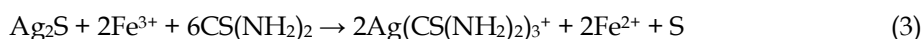
Cyanidation is the conventional hydrometallurgical method of extraction where cyanide ion is the leaching agent and oxygen the oxidant. For both native gold (Au) and native silver (Ag) the corresponding reactions –where M stands for the noble metal- are well known (Jiang et al., 2015):



For silver sulfide cyanidation, the corresponding equation is the following (Jiang et al., 2015):



On the other hand, thioureation is an alternative leaching method in which thiourea is the leaching agent and Fe(III) ion is the oxidant. The reaction occurs according to the following equation (Bruckard et al. 1993):



Given the complexity of the matrix hosting the silver-containing mineralogical species, and the inherent complexity of leaching operations, several strategies are needed to start obtaining information of such systems in a step-wise manner. One of them is by performing leaching experiments on “ideal” minerals such as  $Ag_2S$  (Xie and Dreisinger, 2007; Jiang et al., 2015). Another approach is to study the solid/fluid interfaces at the atomic level by means of first-principles analyses –based on numerical solutions of the quantum mechanical equations- such as Density Functional Theory (DFT). DFT-based analysis provides accurate qualitative and quantitative information, and it has the ability to guide the experiment and improve the interpretation of experimental results (Toulhoat et al., 2005). In mineral processing, studies applying DFT (Feng et al., 2017) and in combination with experimental techniques (Feng et al., 2017) are becoming common for interpreting complex processes in flotation. However, to the best of our knowledge, no such studies exist yet for leaching of silver-bearing sulfides as it relates to reactivity trends which is the focus of the present work.

In this paper, we propose a framework for modeling reactions of cyanide and thiourea with acanthite ( $Ag_2S$ ) considering solvent effects.  $Ag_2S$  is a good representative system given its high silver content and simple structure that facilitates using higher levels of theory. We use DFT to evaluate the reaction energetics and probe reactivity trends comparing the reaction energetics with the respective experimental data on maximum silver extraction.

## 2. Materials and methods

### 2.1. Computational details

All calculations were carried out with the Gaussian 09 suite of programs (Frisch et al., 2009). All model species were calculated as singlets except Fe(II) (spin state  $S=2$ ), Fe(III) (spin state  $S=5/2$ ) and oxygen (spin state  $S=1$ ).

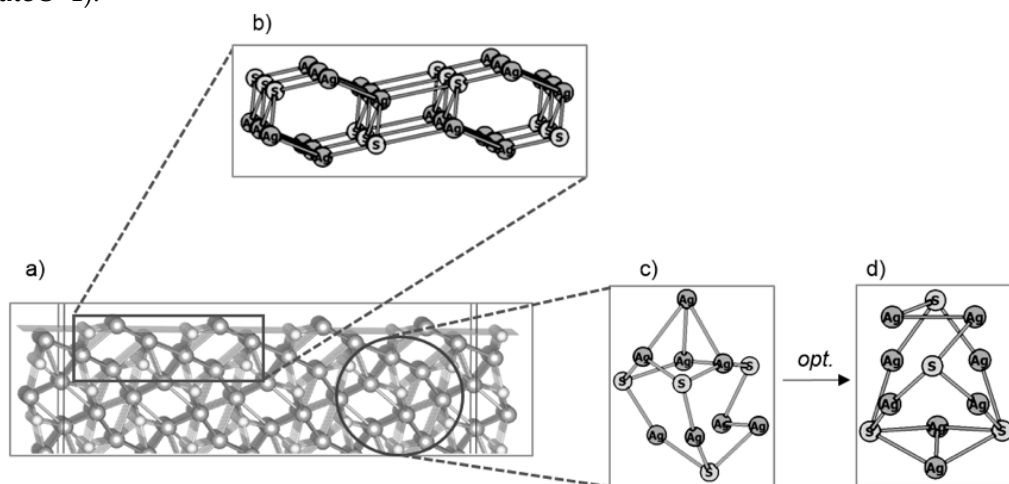


Fig. 1. (a) Side view of an acanthite crystal showing cleavage plane (001). (b) Cluster model ac(001) of stoichiometry  $Ag_{24}S_{12}$  cut from the acanthite crystal. (c) Twelve neighboring atoms extracted from the acanthite crystal prior to optimization. (d) Optimized nanocluster model of stoichiometry  $Ag_8S_4$

Two distinct cluster models for acanthite were built from the corresponding acanthite crystal (Frueh Jr., 1958) using the VESTA (Momma and Izumi, 2008) and Chemcraft (Zhurko and Zhurko, 2016)

programs. The first one, -ac(001) model- was an acanthite(001) surface (Fig. 1b), whereas the second one -nanocluster model- was a minimum energy structure (Fig. 1d) that resulted from the optimization of twelve neighboring atoms -eight silver and four sulfur atoms, according to Ag/S ratio in  $\text{Ag}_2\text{S}$ - extracted from the acanthite crystal as displayed in Fig. 1c. The optimized "nanocluster" model was determined to be at least a local minimum among three clusters of similar stoichiometry calculated at B3PW91/6-31+g(d) level of theory in the gas phase.

The detailed mechanism by which acanthite leaches with both cyanide and thiourea at the molecular level is -to the best of our knowledge- unknown. Given that we are interested in thermodynamics of each global leaching reaction, specifically their Gibbs energies of reaction, we only need a proper approximation of the initial and final steps as we argue below.

Upon reaction with the leaching agents, leaching ionic products are expected to diffuse into the bulk aqueous phase. However, the reactants conversion may be far from being complete which would imply that an unreacted amount of acanthite may remain in the solid phase once leaching -in the macroscale- stops. With this in mind, we envisioned a procedure (Fig. 2) by which the acanthite surface in contact with a water molecule (the initial step) may interact with the ligands (either cyanide or thiourea). Then, after water is removed and the ligand is bound by a silver surface atom, we removed such silver atom and also its closest silver and sulfur neighboring atoms. Finally, a water molecule was placed and optimized in the empty space left after removal of the three removed atoms to represent the unreacted acanthite surface once a mole of  $\text{Ag}_2\text{S}$  is converted into products. It should be noticed that in order to avoid unrealistic distortions of the surface, no optimization of cluster coordinates was done for the ac(001) model.

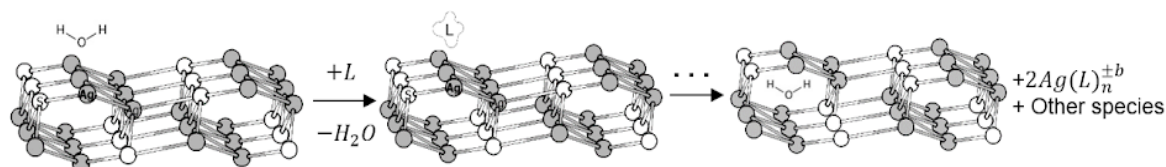
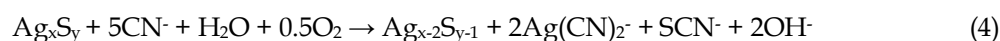


Fig. 2. Modeling the extraction process of 2 silver and 1 sulfur atoms of the acanthite surface exemplified with our model ac(001). L: leaching agent. For cyanidation,  $n=2$  and  $b=-1$ , and for thiourea  $n=3$ ,  $b=+1$ . Eqn 13 and Eqn 15 provide details of the reactions with cyanide and thiourea, respectively

Given the incomplete conversion of acanthite argued above, Eqns. 2 and 3 cannot properly describe the sought leaching processes. Thus, we propose that cyanidation and thiourea are better modeled by the equations shown below:



where  $x$  and  $y$  are the number of silver and sulfur atoms in each cluster model, respectively and with  $x = 2y$ .

Calculating Gibbs energies of reaction from first principles is challenging because reactions of particular interest to hydrometallurgy take place at finite temperatures and imply contact of an aqueous solution with a solid surface. The typical treatment of reactions in solutions is in terms of a thermodynamic cycle (Hellweg and Eckert, 2017) although other authors suggested an alternative method based on the optimization of structures in solvent media rather than in gas phase (Ho, 2015; Ho and Ertem, 2016). This was the approach followed in this work. Both methods are totally equivalent.

Before calculating the standard Gibbs energy of reaction ( $\Delta G^\circ$ ), the Gibbs energy of formation for each of the involved species should be calculated first. First, let us consider that each species in Eqns. 4 or 5 -whether reactant or product- is complexed to a given number of explicit water molecules. Thus, after including these species in those equations, water must be added to keep the equation balanced. This is readily accomplished by adding a  $(\text{H}_2\text{O})_8$  water cluster -approach that resembles one previously followed by Bryantsev et al. (Bryantsev et al., 2008)- to either the left or right side of Eqns 4 and 5 and balancing the equations. Water clusters are used consistently in all our work. All structures and energies were calculated within the DFT framework given its success in predicting structures and

properties of similar systems with many heavy atoms specifically metal and metal chalcogenide clusters (Fernando et al., 2015).

In this work, the B3PW91 functional (Becke, 1993) with an ultrafine integration grid was used taking into account solvent effects by using the IEFPCM implicit solvation model (Tomasi et al., 2005; Mennucci, 2012). All structure optimizations were followed by vibrational frequency calculations. Such calculations had two purposes: first, aid in proving stationary points by verifying absence of imaginary frequencies and second, obtain thermal contributions at 298 K and 1 atm to evaluate the Gibbs free energies within the ideal gas/rigid rotor/harmonic oscillator (IGRRHO) approach –as implemented in Gaussian 09 (Frisch et al., 2009).

Three different basis sets were used (hereafter named BS1, BS2 and BS3), all of them with inclusion of diffuse functions for adequate description of anions. The first one (BS1) combined the 6-31+g(d) basis set for atoms of elements lighter than iron and (Hay and Wadt, 1985) effective core potentials (ECPs) with double zeta basis set (LANL2DZ) for Fe and Ag. The second one (BS2) combined the 6-311+g\* basis set for elements lighter than Ag and LANL2DZ only for Ag, whereas the third one (BS3) combined the aug-cc-PVDZ basis set for elements lighter than Ag and LANL2DZ for silver.

Two distinct levels of theory B3PW91/BS1 (LT1) and B3PW91-D3/BS3//B3PW91/BS2 (LT2), respectively were used. For the LT1 level, optimization and vibrational frequency calculations were done with B3PW91 and basis set BS1. On the other hand, LT2 level of theory entails optimization and vibrational frequency calculations with B3PW91 and basis set BS2 followed by a single point calculation with B3PW91, an empirical dispersion correction based on Grimme's zero damping D3 method (Grimme et al., 2010) –to account for van der Waals interactions- and basis set BS3.

It should be kept in mind that full optimization was done for all cyanidation and thioureaation reactant and product species needed, whereas only partial optimization of water, thiourea and cyanide were carried out over the ac(001) model because all coordinates of such model were kept fixed during the optimization. The impact of this modeling approach will be assessed in a follow up paper.

## 2.2. Experimental details

All reagents were used without further purification. Acanthite (Sigma Aldrich, 99.9% pure, molar mass = 247.8, 87.06 % Ag and 12.94% S (w/w)) was used as received (it passed mesh 270). For thioureaation tests, thiourea (Sigma Aldrich, 99.0% pure), ferric sulfate (Sigma Aldrich, 97.0% pure) and sulfuric acid (MERCK, 97.0% pure) were used, whereas for cyanidation tests sodium cyanide (Sigma Aldrich, 95% pure) in appropriate amounts was added to a solution whose pH was adjusted with commercial calcium hydroxide to ensure a pH in the range 10.5 – 11. SAFETY NOTE: Working with sodium cyanide is dangerous and caution should be exercised at all times. In particular, solutions should be always at pH above 10 to avoid the formation of gaseous HCN. For free thiourea determination in the thioureaation liquor, samples were titrated with potassium iodate (JT Baker, 99.4% pure) and starch as indicator whereas free cyanide determination in cyanidation liquor was performed by titration of samples with silver nitrate (J.A. Elmer, 99.8% pure) and potassium iodide as indicator. For all tests, deionized water was used.

Thioureaation experiments were conducted with 0.1 g of acanthite in 100 cm<sup>3</sup> of (corresponding to 0.1 % w/v) solution with 65.7 mmol/L and 6.3 mmol/L of thiourea and ferric sulfate (Fe<sub>2</sub>(SO<sub>4</sub>)<sub>3</sub>), respectively at room temperature whereas cyanidation experiments were conducted with same mass of acanthite (0.1% w/v) in 100 cm<sup>3</sup> of a NaCN solution of 61.2 mmol/L at room temperature. Both suspensions were agitated at 300 RPM with a flocculator JLT4 Velp Scientifica. The pH of solutions was monitored with a pH-meter Thermo Scientific/Orion G02558 and remained close to 1, as used on previous thioureaation studies (Gašpar et al., 1994; Baláž et al., 1996) for thioureaation throughout leaching and in the range 10.5-11 for cyanidation.

Both cyanidation and thioureaation of acanthite were performed for 4 hours. Samples of leaching liquor were taken at one, two, three and four hours in order to determine both the bulk concentration of leaching agents as well as the concentration of silver in the liquor, which was measured via Atomic absorption spectroscopy (AAS) in a Shimadzu AA7000 spectrometer.

### 3. Results and discussion

#### 3.1. Standard reduction potential calculation for selected relevant aqueous phase reduction reactions

Validation of levels of theory used in this study was done by calculating aqueous-phase reduction potentials of relevant reactions. This is because reduction potentials are regarded as good target properties to assess suitability of electronic structure methods and implicit solvation models (Isegawa et al., 2016). Explicit water molecules were added because their use along with continuum solvation models improves the accuracy of predicted redox potentials (Isegawa et al., 2016).

Standard reduction potentials ( $E^0$ ) of representative reactions that occur during the leaching processes under study are obtained from the calculation of their corresponding standard Gibbs energy of reaction ( $\Delta G^\circ$ ) as follows:

$$\Delta G^\circ = -nFE^\circ \quad (6)$$

where  $n$  stands for the number of electrons exchanged and  $F$  for the Faraday constant. The three representative reactions for which the relevant Gibbs energies of formation were calculated for all species involved in them are as follows:



Great caution should be exercised whenever thermodynamic parameters are estimated from published thermodynamic tables. Large errors could arise from estimation of these parameters when values for individual species are taken from different sources. This is because of the disparity of the values for the obtained standard Gibbs energies of formation, as illustrated by the values for the  $\text{Fe}^{3+}$  and  $\text{Fe}^{2+}$  derived from high-quality publications such as the NBS tables (Wagman et al., 1982):  $-4.7$  kJ/mol and  $-78.90$  kJ/mol for  $\text{Fe}^{3+}$  and  $\text{Fe}^{2+}$ , respectively, compared to other sources ( $-16.23$  kJ/mol and  $-90.5$  kJ/mol) for the same ions (Parker and Khodakovskii, 1995). However, it is apparent that the Gibbs energy difference –related to standard cell potential– is only  $0.07$  kJ/mol which makes  $E^0$  a better property to validate our method.

One of the simplest methods to predict reduction potentials computationally is by adding the half-cell reaction of the reference electrode to the redox reaction of interest (Arumugam and Becker, 2014). Therefore, if we add the standard hydrogen electrode (SHE) half-cell reaction to eqns. 7, 8 and 9, their corresponding complete redox reactions are the following:



Next, the standard Gibbs energy of reaction ( $\Delta G^\circ$ ) for each of the reactions described by eqns. 10, 11, and 12 is calculated from the standard Gibbs energy of formation ( $\Delta G_f^\circ$ ) of each of the involved species therein. A certain number of water molecules of solvation surrounded the ions and this number was estimated in the following manner: i) For  $\text{H}^+$  and  $\text{OH}^-$ , water molecules were added sequentially until reaching the smallest possible error at the highest level of theory for  $E^0$  of the  $\text{O}_2/\text{OH}^-$  redox pair respect to the respective value estimated from tables; ii) For the  $\text{Fe}^{3+}/\text{Fe}^{2+}$  redox pair, two solvation shells were found to lower the error for  $E^0$  respect to the case with one solvation shell; iii) For the pair  $\text{SCN}^-/\text{S}^{2-}$ , several solvated structures were calculated for the species involved therein ( $\text{SCN}^-$ ,  $\text{S}^{2-}$  and  $\text{CN}^-$ ) so as to yield the lowest possible error for  $E^0$ . In all these cases, the error was estimated with reference to values of  $E^0$  computed from Gibbs energies of formation for ions taken from thermodynamic tables. With these number of solvation water molecules,  $E^0$  was also calculated at the B3PW91/BS1 level of theory. The results are shown in Table 1.

Methods that combine a single point energy calculation at a high level of theory and geometry optimizations with vibrational analysis with less expensive methods are regarded as a good strategy to make predictions of standard Gibbs energies of reaction (Hellweg and Eckert, 2017) –and its related property  $E^0$ . Our calculations (see Table 1) reveal that a significant improvement is achieved for the

one-electron reduction potential of  $\text{Fe}^{3+}$  to  $\text{Fe}^{2+}$  since the difference with estimates from tables decreases from 0.90 V to 0.23 V when comparing results from the two levels of theory. This improvement is more modest for the four-electron oxygen reduction (from 0.44 V to 0.31 V) and for the two-electron reduction of  $\text{SCN}^-$  to  $\text{S}^{2-}$  (from 0.53 V to 0.32 V). Nonetheless, it is observed that at the higher level of theory all redox pairs are predicted in their right place (above or below) respect to the SHE.

Table 1. Calculated standard cell potentials ( $E^\circ$ , in V) and standard Gibbs energies of reaction ( $\Delta G^\circ$ , in kJ/mol) for relevant redox pairs in cyanidation and thioureaation

Redox Pair	$\text{Fe}^{3+}/\text{Fe}^{2+}$		$\text{O}_2/\text{OH}^-$		$\text{SCN}^-/\text{S}^{2-}$	
	$E^\circ$	$\Delta G^\circ$	$E^\circ$	$\Delta G^\circ$	$E^\circ$	$\Delta G^\circ$
LT1 <sup>a</sup>	+1.67	-160.8	-0.03	11.5	-1.40	270.2
LT2 <sup>b</sup>	+1.00	-96.7	+0.10	-36.8	-1.19	230.6
Tables <sup>c</sup>	+0.769	-74.2	+0.409	-154.7	-0.872	165.5

<sup>a</sup>LT1: calculated at the B3PW91/BS1 level of theory

<sup>b</sup>LT2: calculated at the B3PW91-D3/BS3//B3PW91/BS2 level of theory

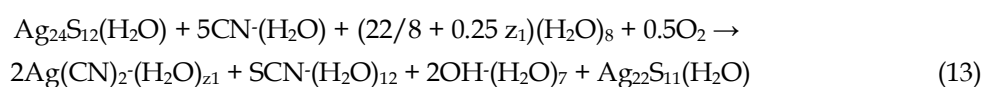
<sup>c</sup>estimated from Gibbs energies of formation found in NBS tables (Wagman et al. 1982)

Overall, it can be realized that the absolute value of the difference between the calculated  $E^\circ$  at level of theory LT1 and the experimental  $E^\circ$  is large, ranging from 0.44 to 0.90 V. Level LT2 yields lower errors ranging from 0.23 to 0.31 V which are comparable with the errors expected for one-electron reduction potentials for transition-metal containing complexes which ranges 0.23 to 0.29 V (Uudsemaa and Tamm, 2003; Liang et al., 2017). Thus, our higher level of theory LT2 is found adequate for the reactions being studied.

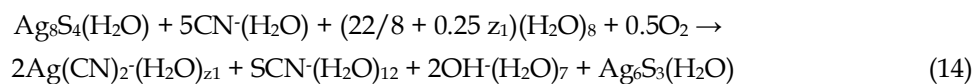
### 3.2. Interaction of leaching agents with acanthite and standard Gibbs energy of reaction ( $\Delta G^\circ$ ) for cyanidation and thioureaation

Both leaching equations (eqns 2 and 3) should be modified to account for incomplete reaction (yielding eqns 4 and 5, respectively) as well as to properly model the solvent effect. In the previous section, a proper number of solvation waters for some of the species involved in these leaching reactions was set to 12 for  $\text{SCN}^-$ , 18 for both  $\text{Fe}^{3+}$  and  $\text{Fe}^{2+}$ , 7 for  $\text{OH}^-$  and 1 for  $\text{CN}^-$ .

Therefore, the model equation for computing  $\Delta G^\circ$  for cyanidation with the ac(001) model is:

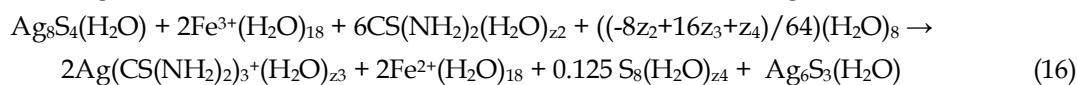
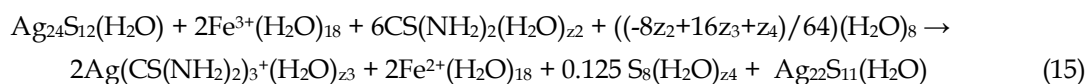


and the corresponding balanced equation to compute  $\Delta G^\circ$  for cyanidation with the nanocluster model is:



where  $z_1$  is the number of water molecules solvating dicyanoargentate(I) ion. For both equations, the corresponding  $\Delta G^\circ$  was calculated for five different solvated  $\text{Ag}(\text{CN})_2^-$  structures ( $z_1 = 1, 2, 5, 10, 18$ ).

Analogous equations for thioureaation for the ac(001) and nanocluster models are defined also as follows:



where  $z_2$ ,  $z_3$  and  $z_4$  are the number of water molecules solvating thiourea, tris(thiourea)silver(I) ion and sulfur ( $\text{S}_8$ ), respectively. For both equations, the corresponding  $\Delta G^\circ$  was calculated for all combinations of four different structures for thiourea ( $z_2 = 0, 2, 4, 6$ ), four for tris(thiourea)silver(I) ( $z_3 =$

0, 2, 3, 6) and two for sulfur ( $S_8$ ) ( $z_2 = 1, 2$ ). Results for the average  $\Delta G^\circ$  based on the leaching model equations outlined above are shown in Table 2.

Both reactions are predicted to be exergonic in agreement with the trend inferred from the estimates from thermodynamic tables. A fair agreement is found between the estimated  $\Delta G^\circ$  from tables and our DFT calculations for cyanidation on the nanocluster model. This is not the case for thioureaation for which a larger deviation is observed for both models. This may be due to the fact that the value (-103.5 kJ/mol) from tables was estimated from Gibbs energies of formation ( $\Delta G_f^\circ$ ) extracted from two different references (Wagman et al., 1982; Gašpar et al., 1994) whereas this was not the case for cyanidation. Moreover, it should be noted that the  $\Delta G^\circ$  computed from values taken from thermodynamic tables unrealistically assume the bulk crystal rather than the surface to be a reactant in the studied reactions.

Table 2. Average standard Gibbs energy of reaction ( $\Delta G^\circ$  in kJ/mol) at the B3PW91-D3/BS3//B3PW91/BS2 level of theory for reactions and models tested in kJ/mol of  $Ag_2S$  leached according to eqns 13-16

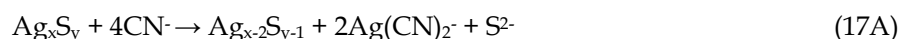
	Cyanidation		Thioureaation	
	ac(001)	nanocluster	ac(001)	nanocluster
Our work	-27.4	-176.1	-280.9	-298.5
From tables <sup>a</sup>		-195.2		-103.5

<sup>a</sup>estimated from Gibbs energies of formation found in literature (Wagman et al., 1982; Gašpar et al., 1994)

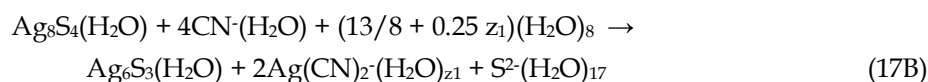
Table 2 also reveals that for the same leaching reaction there is a relationship between the magnitude of the calculated Gibbs energies of reaction and the model size and kind. Both cluster models seek to emulate the acanthite real surface. In the ac(001) cluster model, the surface atoms are fixed to emulate an infinite surface so that any result computed with it will be affected by the finite size effect and absence of surface vibrations. On the other hand, the nanocluster model -with multiple exposed facets- could represent a very reactive surface because of its smaller size and unfixed atoms. Moreover, metal sulfide nanoparticles (Wang et al., 2013; Jiang et al., 2018) are regarded as more reactive as their size decreases, in agreement with the trend suggested by our models: the smaller the model, the larger the absolute value of Gibbs energies is. Nonetheless, the true surface would exhibit periodicity and regarding reactivity with either leaching agent, its Gibbs energy could be an intermediate between the two scenarios shown. Therefore, experimental reactivity trends are realized by using both models.

### 3.3. Model predictions for leaching of acanthite with and without oxidant

Although high exergonicity does not imply fast kinetics, it is interesting to note that dissolution of  $Ag_2S$  by cyanide in the absence of oxygen is expected to occur at a negligible extent (Xie and Dreisinger, 2007). Thus, we propose silver sulfide dissolution by cyanide without oxygen to be as follows:



and after applying a similar approach to what was shown in the previous section, with our nanocluster model, the above equation becomes:



where  $z_1$  is the number of solvation water molecules for dicyanoargentate(I) ion as mentioned previously.

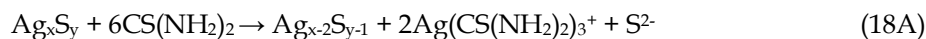
Given that the nanocluster model places an upper boundary for thermodynamic feasibility of such reaction, the calculated average standard Gibbs energy of reaction is +72.9 kJ/mol. This shows a clear endergonic process in the same order of magnitude than what it is expected from  $\Delta G^\circ$  that arises from combining the known  $K_{sp}$  for  $Ag_2S$  ( $\log K_{sp} = -50.1$ ) and the stability constant for the dicyanoargentate complex ( $\log \beta = 20.23$ ) adding up to +55.5 kJ/mol. Our DFT calculated value (+72.9 kJ/mol) for the same amount is within the error found (8-17 kJ/mol) in an ab-initio study on Gibbs energy of

solvation of metal ion complexes (Gutten and Rulíšek, 2013) Therefore, it is apparent that eqn 17A is a less likely –perhaps even unfeasible– pathway for cyanidation than such proposed by eqn 4. This result highlights the need for oxygen to drive cyanidation as it is well known from common hydrometallurgical practice.

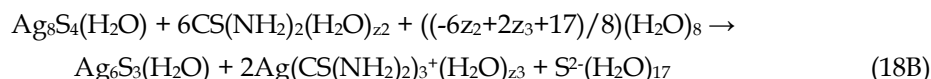
Table 3. Average standard Gibbs energy of reaction ( $\Delta G^\circ$ ) calculated at the B3PW91-D3/BS3//B3PW91/BS2 level of theory for cyanidation and thioureaation in the presence and absence of oxidant in kJ/mol of  $\text{Ag}_2\text{S}$  leached according to Eqns 14, 16, 17B and 18B, using the nanocluster model as an upper boundary for thermodynamic feasibility

	Cyanidation	Thioureaation
With oxidant	-176.1	-298.5
Without oxidant	+72.9	+123.7

In the same manner, experimental studies done with thiourea highlight the importance of the oxidant agent ( $\text{Fe}^{3+}$ ) to drive the reaction (Bruckard et al., 1993; Gašpar et al., 1994). Our own experimental results (not reported here) indicate that no meaningful dissolution of silver sulfide occurs in the absence of  $\text{Fe}^{3+}$  since only 0.8% of Ag was recovered using 0.1g of acanthite in 100 cm<sup>3</sup> of 13.1 mmol/L of thiourea solution and pH = 1 after four hours of leaching. This could be either because of slow kinetics or a less favorable thermodynamics when compared to the process when  $\text{Fe}^{3+}$  is used as oxidant. To test the latter hypothesis, an analogous reaction to eqn. 17A was proposed for thioureaation in the absence of  $\text{Fe}^{3+}$  as follows:



which by following our approach with the nanocluster model becomes:



where  $z_2$  and  $z_3$  are the number of solvation water molecules for thiourea and tris(thiourea)silver(I), respectively as shown previously.

The calculated  $\Delta G^\circ$  of reaction was computed to be +123.7 kJ/mol revealing a clear endergonic process.

Taken together, some interesting patterns emerge from our calculations: first, they emphasize the importance of the oxidants to promote the exergonicity of a surface reactive process such as those found in mineral processing; second, that the higher the  $\Delta G^\circ$  of a given leaching reaction on acanthite, the lower the extent of leaching, provided no kinetic control of the reaction exists. Therefore, we turn our attention to experimental leaching tests with synthetic acanthite to find whether this insight holds or not by seeking a relationship between  $\Delta G^\circ$  of a leaching reaction and the maximum experimental extraction of silver from acanthite, provided these leaching reactions are thermodynamically-controlled processes.

### 3.4. Relationship between DFT-based Gibbs energy of reaction and maximum silver experimental extraction

Meaningful comparison of leaching efficiency of thioureaation and cyanidation is possible only if similar percentage of solids and molar concentration of leaching agents are used. Thus, the results of our experiments performed at similar molarity of leaching agent (61 mM for cyanide vs. 65 mM for thiourea) and same percentage of solids (0.1% w/v) are shown in Figure 3.

Figure 3 shows that thiourea extracts more silver from acanthite until the fourth hour. During the first hour, thiourea extracts silver 4.6 times faster than cyanide. Then, the acanthite leaching rate decreases and for the fourth hour the silver extraction with thiourea decreases and becomes lower than that of cyanide, possibly due to preg-robbing of silver species on sulfur species such as elemental sulfur, a byproduct of thioureaation or sulfur deposition on acanthite surface precluding further acanthite dissolution into the bulk solution.



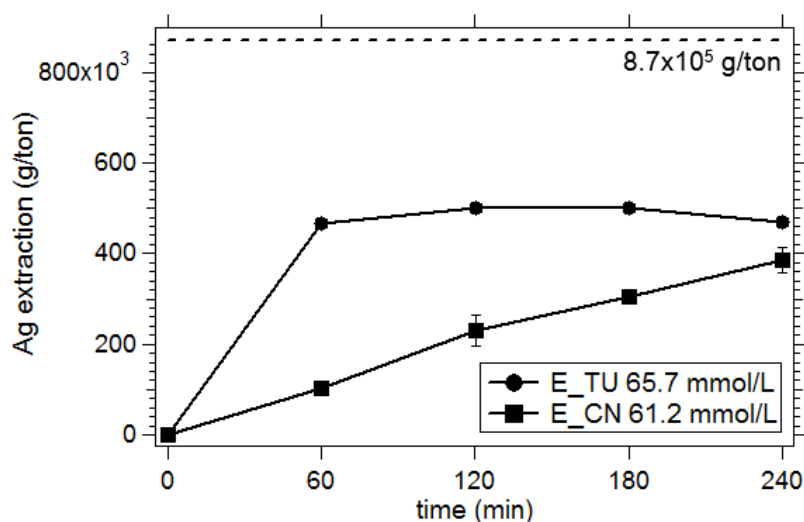


Fig. 3. Silver extraction (g Ag per Mg of acanthite) by thiourea and cyanidation at similar molar concentration and % solids (0.1% w/v). E\_TU 65.7 mmol/L: cumulative silver extracted with thiourea (TU), E\_CN 61.2 mmol/L: cumulative silver extracted with sodium cyanide (NaCN). All experiments were done in similar conditions of stirring, temperature and amount of acanthite. Experiments were done in duplicate. Dashed line shows theoretical silver content in 1 Mg (1 ton) of acanthite

For thiourea, given that no additional silver is extracted between the second and third hour of leaching, equilibrium between solid and liquid phases is likely reached. This in turn implies that maximum silver extraction could be achieved by the third hour, despite the slight decrease in extraction observed beyond this hour. Regarding cyanide, a maximum silver extraction is observed (Figure 3) by the fourth hour. However, from the experiments, it is unclear how this trend would continue after 4 hours.

Table 4 shows the maximum amount of silver leached at the third hour for thiourea and at the fourth hour for cyanidation, alongside the DFT-calculated standard Gibbs energy of reaction ( $\Delta G^\circ$ ) and the Gibbs energy of reaction ( $\Delta G$ ) for non-standard conditions which were room temperature, atmospheric pressure of 1 atm and molar concentration of soluble species different from 1M. Because no concentration of species was measured throughout the experiments (NOTE: for cyanidation, OH<sup>-</sup> concentration was inferred from the pH and for O<sub>2</sub> the corresponding partial pressure was taken into account), the concentrations of reactants and products has been calculated by considering each reaction proceeds according to the stoichiometry specified in eqns 2 and 3. Then, by assuming Nernstian behavior of the reactive systems at the third hour for thiourea and at the fourth hour for cyanidation the corresponding  $\Delta G$  for each reaction is calculated considering the aforementioned reactant and product concentrations.

Table 4 shows that based on the DFT-calculated  $\Delta G^\circ$  of the corresponding leaching reactions, the more exergonic the leaching process is, the more silver is extracted from acanthite, provided no kinetic control operates. Interestingly, this trend is observed not only with calculations based on the nanocluster model but also with the ac(001) model. The same trend is observed considering the non-standard Gibbs energies of reaction based on DFT-calculated values of  $\Delta G^\circ$ . Thus, it is apparent that both  $\Delta G^\circ$  and  $\Delta G$  are qualitative suitable predictors of the maximum extent of leaching of acanthite by thiourea and cyanide.

This work has revealed interesting insights. However, in order to apply this new insight to a different scale, not only more testing would be needed to extend our rationale to the assessment of the performance of other alternative leaching agents such as thiosulphate, thiocyanide and others- but also weighing in additional factors that must be reckoned in greater depth. These factors include concentration of leaching liquor species, presence of gangue minerals and other mineralogical species, mode of leaching, and others. Possibly a multiscale modeling approach, where the DFT results could be used in mesoscopic and/or continuum models would be of great utility to extend the results to macroscopic analysis.

Table 4. DFT-calculated standard Gibbs energy of reaction ( $\Delta G^\circ$ ) at the B3PW91D3/BS3//B3PW91/BS2 level of theory, Gibbs energy of reaction based on such values ( $\Delta G$ ) and maximum percentage of silver extracted

	Cyanidation	Thioureaation
Maximum % of silver extracted <sup>a</sup>	44.3%	57.5%
$\Delta G^\circ$ (kJ/mol) (DFT)	-27.4 <sup>c</sup>	-280.9 <sup>c</sup>
	-176.1 <sup>d</sup>	-298.5 <sup>d</sup>
$\Delta G$ (kJ/mol) (DFT-based) <sup>b</sup>	-59.2 <sup>c</sup>	-354.1 <sup>c</sup>
	-207.9 <sup>d</sup>	-371.7 <sup>d</sup>

<sup>a</sup>assuming maximum percentage of recovery of silver is achieved at third hour of leaching for thiourea and fourth hour for cyanidation

<sup>b</sup>calculated by assuming stoichiometry determines species concentrations when maximum silver percentage recovery is achieved.

<sup>c</sup>calculations done with model ac(001)

<sup>d</sup>calculations done with nanocluster model

#### 4. Conclusions

Reactions of hydrometallurgical value such as the leaching of a silver mineral by either cyanide or thiourea were studied combining first principles calculations and experiments for the first time. DFT calculations of cluster models considering solvent effects predicted both leaching reactions to be exergonic. Their Gibbs energies of reaction –at the conditions the experiments were done- are of the same order of magnitude than estimates from thermodynamic tables. and the study demonstrated the important role of the oxidant to make the leaching reactions thermodynamically feasible, in agreement with experimental observations. Small scale experiments also reveal that a higher percentage of silver is extracted by thioureaation than by cyanidation at same percentage of solids, temperature and similar molar concentration of leaching agent.

Taken together our results show that the more spontaneous the corresponding leaching reaction is, the higher the extracted percentage of silver. However, thoughtful consideration of additional factors is needed before generalizing our results to other mineral/leaching agent systems. These factors include concentration of leaching liquor species, presence of gangue minerals and other mineralogical species, and others.

#### Acknowledgments

This work has been supported by Peru's Consejo Nacional de Ciencia y Tecnología (CienciActiva – CONCYTEC) and the British Embassy in Lima [contract numbers 154-2015 and 002-2016]. Portions of this research were conducted with the advanced computing resources provided by Texas A&M High Performance Research Computing. Ms. Karinna Visurraga (UTEC) is kindly acknowledged for administrative support.

#### References

- AÇMA, E., ARSLAN, F., WUTH, W., 1993. *Silver extraction from a refractory type ore by thiourea leaching*. Hydrometallurgy 34, 263–274.
- ALP, I., CELEP, O., PAKTUNÇ, D., THIBAUT, Y., 2014. *Influence of potassium hydroxide pretreatment on the extraction of gold and silver from a refractory ore*. Hydrometallurgy 146, 64–71.
- ARUMUGAM, K., BECKER, U., 2014. *Computational Redox Potential Predictions: Applications to Inorganic and Organic Aqueous Complexes, and Complexes Adsorbed to Mineral Surfaces*. Minerals 4, 345–387.
- AYLMORE, M. G., MUIR, D. M., AYLMOORE, M. G., 2001. *Thiosulfate Leaching of Gold—a Review*. Miner Eng 14, 135–174.
- BALÁŽ, P., FICERIOVÁ, J., ŠEPELÁK, V., KAMMEL, R., 1996. *Thiourea Leaching of Silver from Mechanically Activated Tetrahedrite*. Hydrometallurgy 43, 367–377
- BECKE, A. D., 1993. *Density-functional thermochemistry. III. The role of exact exchange*. J. Chem. Phys. 98:5648–5652.

- BRUCKARD, W. J., SPARROW, G. J., WOODCOCK, J. T., 1993. *Gold and silver extraction from Hellyer lead-zinc flotation middlings using pressure oxidation and thiourea leaching*. Hydrometallurgy 33, 17–41.
- BRYANTSEV, V. S., DIALLO, M. S., GODDARD III, W. A., 2008. *Calculation of Solvation Free Energies of Charged Solutes Using Mixed Cluster/Continuum Models*. J. Phys. Chem. B 112, 9709–9719.
- CELEP, O., ALP, I., PAKTUNÇ, D., THIBAUT, Y., 2011. *Implementation of sodium hydroxide pretreatment for refractory antimonial gold and silver ores*. Hydrometallurgy 108, 109–114.
- EMERY-TRINDADE, R., 1994. *Tiouréia e bromo como lixiviantes alternativos à cianetação de ouro*. CETEM/CNPq, Rio de Janeiro.
- FENG, Q., WEN, S., DENG, J., ZHAO, W., 2017. *DFT Study on the Interaction between Hydrogen Sulfide Ions cerussite (110) surface*. Appl. Surf. Science 396, 920–925
- FENG, Q., WEN, S., DENG, J., ZHAO, W., 2017. *Combined DFT and XPS Investigation of Enhanced Adsorption of Sulfide Species onto Cerussite by Surface Modification with Chloride*. Appl Surf Science 425, 8–15
- FERNANDO, A., WEERAWARDENE, K. L. D. M., KARIMOVA, N. V., AIKENS, C. M., 2015. *Quantum Mechanical Studies of Large Metal, Metal Oxide, and Metal Chalcogenide Nanoparticles and Clusters*. Chem Rev 115, 6112–6216.
- FRISCH, M. J., TRUCKS, G. W., SCHLEGEL, H. B., SCUSERIA, G. E., ROBB, M. A., CHEESEMAN, J. R., SCALMANI, G., BARONE, V., MENNUCCI, B., PETERSSON, G. A., NAKATSUJI, H., CARICATO, M., LI, X., HRATCHIAN, H. P., IZMAYLOV, A. F., BLOINO, J., ZHENG, G., SONNENBERG, D. J., HADA, M., EHARA, M., TOYOTA, K., FUKUDA, R., HASEGAWA, J., ISHIDA, M., NAKAJIMA, T., HONDA, Y., KITAO, O., NAKAI, H., VREVEN, T., MONTGOMERY, J. A., JR., PERALTA, J. E., OGLIARO, F., BEARPARK, M., HEYD, J. J., BROTHERS, E., KUDIN, K. N., STAROVEROV, V. N., KEITH, T., KOBAYASHI, R., NORMAND, J., RAGHAVACHARI, K., RENDELL, A., BURANT, J. C., IYENGAR, S. S., TOMASI, J., COSSI, M., REGA, N., MILLAM, J. M., KLENE, M., KNOX, J. E., CROSS, J. B., BAKKEN, V., ADAMO, C., JARAMILLO, J., GOMPERTS, R., STRATMANN, R. E., YAZYEV, O., AUSTIN, A. J., CAMMI, R., POMELLI, C., OCHTERSKI, J. W., MARTIN, R. L., MOROKUMA, K., ZAKRZEWSKI, V. G., VOTH, G. A., SALVADOR, P., DANNENBERG, J. J., DAPPRICH, S., DANIELS, A. D., FARKAS, Ö., FORESMAN, J. B., ORTIZ, J. V., CIOŚŁOWSKI, J., FOX, D. J., 2013. *Gaussian 09, Revision E.01*. Gaussian, Inc. Wallingford CT
- FRUEH JR., A. J., 1958. *The Crystallography of silver sulfide Ag<sub>2</sub>S*. Zeitschrift fur Krist 110, 136–144
- GAŠPAR, V., MEJEROVICH, A.S., MERETUKOV, M. A., SCHMIEDL, J., 1994. *Practical application of potential-pH diagrams for Au-CS(NH<sub>2</sub>)<sub>2</sub>-H<sub>2</sub>O and Ag-CS(NH<sub>2</sub>)<sub>2</sub>-H<sub>2</sub>O systems for leaching gold and silver with acidic thiourea solution*. Hydrometallurgy 34, 369–381.
- GASPARRINI, C., 1983. *The mineralogy of gold and its significance in metal extraction*. CIM Bull 76, 144–153
- GRIMME, S., ANTONY, J., EHRLICH, S., KRIEG, H., 2010. *A consistent and accurate ab initio parametrization of density functional dispersion correction (DFT-D) for the 94 elements H-Pu*. J Chem Phys 132, 154104–154119.
- GUTTEN, O., RULÍŠEK, L., 2013. *Predicting the stability constants of metal-ion complexes from first principles*. Inorg Chem 52, 10347–10355.
- HAY, P. J., WADT, W. R., 1985. *Ab initio effective core potentials for molecular calculations. Potentials for the transition metal atoms Sc to Hg*. J Chem Phys 82, 270–283.
- HELLWEG, A., ECKERT, F., 2017. *Brick by brick computation of the gibbs free energy of reaction in solution using quantum chemistry and COSMO-RS*. AIChE J 63, 3944–3954.
- HO, J., 2015. *Are thermodynamic cycles necessary for continuum solvent calculation of pK<sub>a</sub>s and reduction potentials?* Phys Chem Chem Phys 17, 2859–2868.
- HO, J., ERTEM, M. Z., 2016. *Calculating Free Energy Changes in Continuum Solvation Models*. J Phys Chem B 120, 1319–1329.
- ISEGAWA, M., NEESE, F., PANTAZIS, D. A., 2016. *Ionization Energies and Aqueous Redox Potentials of Organic Molecules: Comparison of DFT, Correlated ab Initio Theory and Pair Natural Orbital Approaches*. J Chem Theory Comput 12, 2272–2284.
- JIANG, H., XIE, F., DREISINGER, D. B., 2015. *Comparative study of auxiliary oxidants in cyanidation of silver sulfide*. Hydrometallurgy 158, 149–156.
- JIANG, Y., WANG, D., PAN, Z., MA, H., LI, M., LI, J., ZHENG, A., LV, G., TIAN, Z., 2018. *Microemulsion-mediated hydrothermal synthesis of flower-like MoS<sub>2</sub> nanomaterials with enhanced catalytic activities for anthracene hydrogenation*. Front Chem Sci Eng 12, 32–42.
- LA BROOY, S. R., LINGE, H. G., WALKER, G. S., 1994. *Review of gold extraction from ores*. Miner Eng 7:1213–1241.

- LIANG, G., DEYONKER, N. J., ZHAO, X., WEBSTER, C. E., 2017. *Prediction of the reduction potential in transition-metal containing complexes: How expensive? For what accuracy?* J Comput Chem 38:2430–2438.
- LINDSTROM, R. E., SJOBERG, J. J., POOL, D. L., SCHEINER, B. J., 1973. *Extraction of silver from refractory ores*. U.S. Dept. of Interior, Bureau of Mines, Washington, D.C.
- MENNUCCI, B., 2012. *Polarizable continuum model*. Wiley Interdiscip Rev Comput Mol Sci 2, 386–404.
- MOMMA, K., IZUMI, F., 2008. *VESTA: A three-dimensional visualization system for electronic and structural analysis*. J Appl Crystallogr 41:653–658.
- PARKER, V. B., KHODAKOVSKII, I. L., 1995. *Thermodynamic Properties of the Aqueous Ions (2+ and 3+) of Iron and the Key Compounds of Iron*. J Phys Chem Ref Data 24, 1699–1745.
- QIU, X. Y., HU, Z., SONG, B. X., LI, H. W., ZOU, J. J., 2014. *A novel process for silver recovery from a refractory Au-Ag ore in cyanidation by pretreatment with sulfating leaching using pyrite as reductant*. Hydrometallurgy 144–145, 34–38.
- SABA, M., MOHAMMADYUSEFI, A., RASHCHI, F., MOGHADDAM, J., 2011. *Diagnostic pre-treatment procedure for simultaneous cyanide leaching of gold and silver from a refractory gold/silver ore*. Miner Eng 24, 1703–1709.
- SVERDRUP, H., KOCA, D., RAGNARSDOTTIR, K. V., 2014. *Investigating the sustainability of the global silver supply, reserves, stocks in society and market price using different approaches*. Resour Conserv Recycl 83, 121–140.
- TOMASI, J., MENNUCCI, B., CAMMI, R., 2005. *Quantum mechanical continuum solvation models*. Chem Rev 105: 2999–3093.
- TOULHOAT, H., DIGNE, M., ARROUVEL, C., RAYBAUD, P., 2005. *DFT studies of fluid-minerals interactions at the molecular level: Examples and perspectives*. Oil Gas Sci Technol 60, 417–433.
- UBALDINI, S., FORNARI, P., MASSIDA, C., ABBRUZZESE, C., 1998. *An innovative thiourea gold leaching process*. Hydrometallurgy 48, 113–124.
- UUDSEMAA, M., TAMM, T., 2003. *Density-functional theory calculations of aqueous redox potentials of fourth-period transition metals*. J Phys Chem A 107, 9997–10003.
- WAGMAN, D. D., EVANS, W. H., PARKER, V. B., SCHUMM, R. H., HALOW, I., BAILEY, S. M., CHURNEY, K. L., NUTTALL, R. L., 1982. *The NBS tables of chemical thermodynamic properties: selected values for inorganic and C1 and C2 organic substances in SI units*. Phys Chem Ref Data 11: Supplement No. 2, 2.1-2.392.
- WANG, D., WANG, Z., WANG, C., ZHOU, P., WU, Z., LIU, Z., 2013. *Distorted MoS<sub>2</sub> nanostructures: An efficient catalyst for the electrochemical hydrogen evolution reaction*. Electrochem Commun 34, 219–222.
- XIE, F., DREISINGER, D. B., 2007. *Leaching of silver sulfide with ferricyanide – cyanide solution*. Hydrometallurgy 88, 98–108.
- ZHURKO, G. A., ZHURKO, D. A., 2016. *Chemcraft - graphical software for visualization of quantum chemistry computations*. <http://www.chemcraftprog.com>